# Effect of Blue Jets on Atmospheric Composition: Feasibility of Measurement From a Stratospheric Balloon

Laurence Croizé, Sébastien Payan, Jérôme Bureau, Fabrice Duruisseau, Rémi Thiéblemont, and Nathalie Huret

***Abstract*—The feasibility study of the HALESIS (High-Altitude Luminous Events Studied by Infrared Spectro-imagery) project is presented. The purpose of this experiment is to measure the atmospheric perturbation in the minutes following the occurrence of transient luminous events (TLEs) from a stratospheric balloon in the altitude range of 20–40 km. The instrumentation will include a spectro-imager embedded in a pointing gondola. Infrared signatures of a single blue jet were simulated under the assumption of local thermodynamic equilibrium (LTE), and were then compared with a panel of commercially available instrument specifications. The sensitivity of the signatures with a local perturbation of the main vibrational energy level populations of $CO_2$, CO, NO, $O_3$, and $H_2O$ was measured and the infrared signatures of a single blue jet taking into account non-LTE hypotheses were compared with the same panel of commercially available instrument specifications. Lastly, the feasibility of the study is discussed.**

***Index Terms*—Atmospheric chemistry, hyperspectral imagery, transient luminous events (TLEs).**

## I. Introduction

THE OBSERVATION of transient luminous events (TLEs) in the high atmosphere by Franz *et al.* two decades ago [1] and the observation of gamma ray flashes of terrestrial origin [terrestrial gamma flashes (TGFs)] by Fishman *et al.* [2] have evidenced interaction processes between the different atmospheric layers (troposphere, stratosphere, and mesosphere/ionosphere) that had never been studied before. Indeed, the frequency of occurrence of these phenomena over thunderstorm cells is not accurately known [3]–[5] and the impact of the impulsive energy transfer between the troposphere and the highest atmospheric layers on the earth's electrical system has to be studied and quantified.

This paper focuses on an innovative experiment named HALESIS (High-Altitude Luminous Events Studied by Infrared Spectro-imagery) that aims to measure from a stratospheric balloon the effect of TLEs on atmospheric composition and the associated chemistry induced by vibrational excitation. The feasibility study of this experimental project is presented here.

We first present the interest of performing fast and sensitive hyperspectral measurements of the effect of TLEs on the atmospheric composition. Then the HALESIS project and future experiment are described. To establish the feasibility of the project, simulations of the spectral signature of an isolated blue jet were performed in the thermal infrared (TIR) and in the middle infrared (MIR) range. First the perturbed area was considered to be at local thermodynamic equilibrium (LTE). Then the effect of a modification in the main vibrational energy level populations of $CO_2$, CO, NO, $O_3$, and $H_2O$ inside the perturbed area was assessed. The results of the estimation of infrared spectral signatures were compared to the technical capabilities of a panel of infrared spectro-imagers. We conclude not only on the project feasibility, but also on the challenges that lie ahead for an imager perfectly suited to achieve the aims of HALESIS.

## II. Interest of Studying the Atmospheric Composition Perturbation Induced by TLEs

TLEs occur most of the time over thunderstorm clouds. They include different phenomena: Sprites, which extend from 40 to 90 km and can last up to a few tenths of a millisecond [6]; blue jets, which resemble narrow blue columns [6]; elves [7]; luminous halos; and gigantic jets [8]. They appear in different shapes and their color at high altitude is related to the prominence of the first positive band system of molecular nitrogen ($1\mathrm{PG} = \text{First Positive Group of } \mathrm{N_2}$). The phenomenology, morphology, physical, and chemical mechanisms involved as well as the energetic and electric effects of TLEs (both on local and global scales) have been extensively investigated since TLEs were first discovered [9], [10] (see references within for a complete description).

An electrical perturbation caused by a thunderstorm can trigger a discharge above the clouds in the upper layers of the atmosphere. The associated energized electrons excite, ionize, or dissociate the major constituents $N_2$ and $O_2$ of the earth's atmosphere, leading to atomic species ($N(^2D)$, $N(^4S)$, $O(^1D)$, and $O(^1S)$), molecular species ($N_2(C^3\Pi_u)$, $N_2(B^3\Pi_g)$, etc.), or ionic species ($N_2 + (A^2\Pi_u)$). When relaxing to lower energy

Manuscript received July 31, 2014; revised October 01, 2014; accepted November 06, 2014. Date of publication March 08, 2015; date of current version July 30, 2015. This work was supported by the CSTB (Comité Scientifique et Technique Ballon/Balloon Scientific and Technical Committee) of CNES (French space agency).

L. Croizé, S. Payan, and J. Bureau are with UPMC University, Paris, France, also with the Université Versailles St.-Quentin, Versailles, France, and also with CNRS/INSU, LATMOS-IPSL, Paris 75252, France (e-mail: Laurence.croize@latmos.ipsl.fr; sebastien.payan@latmos.ipsl.fr; jerome.bureau@latmos.ipsl.fr).

F. Duruisseau and N. Huret are with the Laboratoire de Physique et Chimie de l'Environnement, CNRS and Université d'Orléans, Orléans 45071, France (e-mail: fabrice.duruisseau@cnrs-orleans.fr; nathalie.huret@cnrs-orleans.fr).

R. Thiéblemont is with the GEOMAR-Helmholtz Centre for Ocean Research Kiel, Kiel 24148, Germany (e-mail: rthieblemont@geomar.de).

Color versions of one or more of the figures in this paper are available online at http://ieeexplore.ieee.org.

Digital Object Identifier 10.1109/JSTARS.2014.2381556

states, visible photons are emitted. This explains the color of the observed phenomena. For example, above 50 km, the red color of sprites arises from the transitions from the $B^3\Pi_g$ to the $A^3\Sigma^+{}_u$ electronic states of $N_2$ (first positive or 1P bands) between 650 and 800 nm, whereas below 50 km red emissions are strongly quenched: blue optical emissions become dominant mainly due to excitation of the second positive band of $N_2(N_2^2P)$ [11], whereas the blue emission of blue jets must have an ionized first negative $N_2^+$ component [12], [13]. Depending on the target study, several modeling studies have been performed in which the number of species considered and energy deposition assumptions may vary from one paper to another (e.g., [14]–[17]).

As they involve a huge transfer of charges between different atmospheric layers, TLEs influence the global atmospheric electricity circuit by charging it (blue jets) or discharging it (gigantic jets) [18]. The formation of oxygen atoms in electronically excited states can also be expected to have an impact on ozone chemistry. Atomic or molecular species excited in electronic or vibrational states can induce various chains of chemical reactions [19] and local enhancements of the concentrations of $O_3$, $NO_x$ (i.e., $NO + NO_2$), and OH.

To better understand the physics of these phenomena, their frequency, and their role in the earth's environment, several projects are being developed worldwide. These projects involve several space experiments: the ISUAL (Imager of Sprites and Upper Atmospheric Lightning) instrument on the Taiwanese–Japanese satellite FORMOSAT, the future French microsatellite TARANIS (Tool for the Analysis of Radiation from Lightning and Sprites [20], and the Japanese ASIM experiment (Atmosphere–Space Interactions Monitor) provided on the ISS (International Space Station) [21].

### A. Previous Observations

The complementary question of how much TLEs influence the atmospheric chemical composition has been addressed by several teams in the past. Pasko *et al.* [10] underlined that atmospheric discharge phenomena (corona discharge, lightning, and TLEs) are known to be significant sources of NO and $NO_2$ in the troposphere and middle atmosphere. They influence the concentrations of ozone ($O_3$) and hydroxyl radicals (OH) so that an appropriate quantification of lightning-produced $LtNO_x$ (including TLE-produced $NO_x$) has become an important issue in studies of the $NO_x$ budget. Based on measurements by the imager ISUAL aboard the FORMOSAT-2 satellite, Chen *et al.* reported occurrence rates of 3.23, 0.50, 0.39, and 0.01 events per minute, respectively, for elves, sprites, halos, and gigantic jets [4]. Estimations of the amount of $LtNO_x$ vary by two orders of magnitude in the range of 1–200 $Tg(N)\ yr^{-1}$, where $1\,Tg(N) = 1012$ g of nitrogen [22]–[25]. In addition, climate change will lead to changes in the frequency and location of thunderstorm activity [26] (and thus in the frequency of TLEs) so that their impact on atmospheric chemistry will have to be reassessed in the future. TLEs have been observed throughout the world, over all continents and several oceans (see [27] and references within [27]).

The local increase in NO and $O_3$ can reach 10% and 0.5%, respectively, at 30 km for blue jets according to Mishin [14]. Theoretical predictions by Hiraki *et al.* estimate a local enhancement of sprite-induced $NO_x$ that may be significant in the range of one to five times the minimum background at 70 km [19].

Peterson *et al.* [28] analyzed $NO_x$ produced by laboratory discharges as a function of pressure, voltage, current, and capacitor energy. They predicted a significant $NO_x$ production when they attempted to reproduce a wide range of stratospheric and mesospheric pressures, covering the range of heights at which blue jets and red sprites have been observed to occur. However, applying their laboratory results to mesosphere conditions, they deduced a small impact on global mesospheric $NO_x$ concentration. Note that these results have large uncertainties (with five orders of magnitude uncertainty) and this work has been strongly criticized by other teams [29], [30] and is still under discussion [31], [32].

Direct measurements—measurements of the local effect induced by an identified TLE—have never been conducted but several teams have attempted to use satellite limb measurements to assess the influence of TLEs on the mean $NO_x$ concentration of the middle atmosphere. Two studies are based on $NO_2$ measurement, which is a good indicator of $NO_x$ production in the stratosphere since $NO_x$ gases are in photochemical equilibrium during the daytime but after sunset NO is quickly converted into $NO_2$ in reaction with $O_3$. Rodger *et al.* [33] used $NO_2$ measurements from GOMOS/ENVISAT (Global Ozone Monitoring by Occultation of Stars onboard *ENVIronment SATellite*) at altitudes from 20 to 70 km, and from selected geographic regions (eight typical regions, including four continental regions: two in north America, one in Africa, and one in south Asia; and four oceanic regions: two in the Pacific, one in the Atlantic, and one in the Indian ocean) during the period July 2002–October 2006. Each region was included in a box $15^\circ$ wide in longitude and $20^\circ$ wide in latitude and was used to examine the significance of NOx production by TLEs at nighttime. The study was based on monthly star occultation limb measurements from typical regions of the globe. They showed that there is no significant impact of red sprites, gigantic jets, or blue jets upon $NO_x$ monthly levels in the stratosphere and mesosphere (from 20 to 70 km of altitude), within the detection levels of the instrument. Arnone *et al.* investigated MIPAS/ENVISAT (Michelson Interferometer for Passive Atmospheric Sounding/ENVISAT) measurements of middle atmospheric $NO_2$ in regions of high likelihood of sprite occurrence during the period August to December 2003 [34]. They adopted the strategy that middle atmosphere MIPAS satellite measurements of $NO_2$ were correlated with ground-based WWLLN (World Wide Lightning Location Network) detections of large tropospheric thunderstorms as a proxy for sprite activity. The instantaneous field of view (IFOV) of MIPAS is about 3 km in height at tangent point and 30 km wide (i.e., along longitude). In latitude, i.e., along the line of sight crossing the atmosphere below 80 km, the MIPAS IFOV footprint is about 1200 km at 52 km height, and 500 km at 60 km height [35]. They found no evidence of any significant impact on a global scale. However, they highlight an indication of a possible

sprite-induced local $NO_2$ enhancement of about 10% at 52 km height in correspondence with active thunderstorms. Their analysis points toward a sprite effect upon the composition of the neutral atmosphere at local scale, with more robust evidence from regions north of the equator (from $5°N$ to $20°N$) [36].

The major difficulty in measuring the impact of TLEs on local atmospheric composition is to link the cause (a TLE occurrence) to the effect (disruption of atmospheric composition). Moreover, the effect of TLEs on vibrational level populations of molecules such as NO, $NO_2$, $O_3$, CO, and $CO_2$ has never been monitored even though it could provide complementary information on the energy deposition.

### *B. Interest of Hyperspectral Imagery for the HALESIS Project*

Depending on their altitude, some TLEs should be accessible to *in situ* balloon-borne measurements but this strategy is not the best approach because 1) it is technically difficult to fly above a thunderstorm; 2) the probability of flying inside the TLE is low; and 3) the study would be restricted to blue jets and gigantic jets due to the maximum altitude of balloons (around 40 km) whereas the study of sprites, halos, and elves is also interesting and complementary.

Remote sensing embedded on a stratospheric balloon is an alternative method that only makes sense if perturbed spectral radiance (i.e., radiances that have been acquired in an area perturbed by a TLE) can be compared with background spectral radiance. Fourier transform in the infrared (FTIR)-based hyperspectral imagery is an alternative efficient method that combines infrared imagery and high-resolution spectroscopy.

For the purposes of HALESIS, the advantage is twofold. The comparison of spectra from central pixels (i.e., perturbed by a TLE) with spectra pixels on the edge (background radiance) provides the intensity of the perturbation, while the second spatial dimension provides access to the vertical distribution of the perturbation.

Some FTIR-based models are commercially available. In the present study, a panel of such instruments was used to establish a set of typical specifications. But there are also some research prototypes that must be mentioned. GLORIA (Gimbaled Limb Observer for Radiance Imaging of the Atmosphere) is a new remote sensing instrument that combines an FTIR spectrometer with a two-dimensional (2-D) detector array in the spectral regions in combination with a highly flexible Gimbal mount. The spectral range of the first instrument version extends from 780 to $1400\,\mathrm{cm}^{-1}$ with a spectral resolution of up to $0.075\,\mathrm{cm}^{-1}$. The technical specifications of this instrument represent the state-of-the-art of IR hyperspectral imagery dedicated to limb sounding [37]. The SYSIPHE (SYstème Spectro-Imageur de mesure des Propriétés Hyperspectrales Embarqué/Spectro-Imaging Inboard System for the Measurement of Hyperspectral Properties) system is the state-of-the-art airborne hyperspectral imaging system in the spectral range from 0.4 to $11.5\,\mu\mathrm{m}$ using a nadir line of sight [38], [39].

The aim of HALESIS is to measure the effect of TLEs on the atmospheric composition in the minutes following the occurrence of a TLE. The chosen strategy is to identify some TLE occurrences from a stratospheric balloon and to infer the local atmospheric composition in the following minutes with an acquisition frequency of about a few hyperspectral cubes every 10 s. This acquisition frequency should make it possible to monitor $NO_2$ but also NO, $NO^+$, and $O_3$ concentration time evolution.

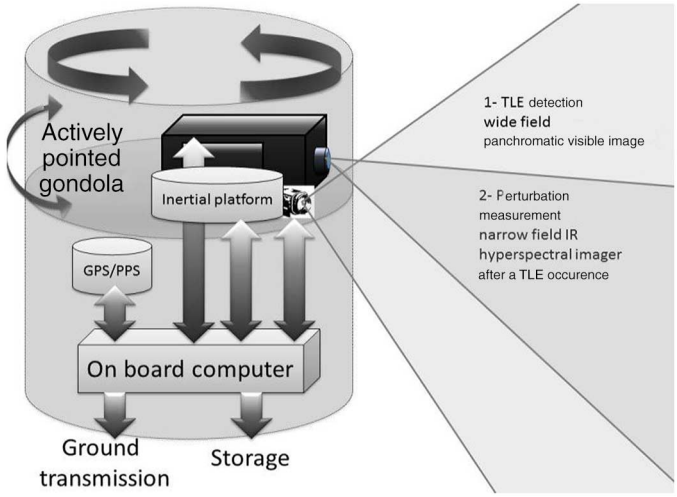


Fig. 1. HALESIS instrument principle.

The HALESIS instrumentation (Fig. 1) will be integrated on a pointing gondola that will ensure that the FOV of the instrumentation remains locked on the direction (thanks to an inertial station) where a TLE occurs. The gondola—built like the SALOMON one [40]—will be prepointed on the direction of the event. Then, a panchromatic low-light camera (typically WATEK WAT-902 ULTIMATE) will be used to detect the TLEs with an acquisition rate of 25 f/s (frames/s). Detection will be done in the visible and near infrared with a wide FOV (typically with a fish-eye lens). The WATEC camera will be used for detection purposes only. For scientific purposes, a more accurate imager can be added for the interpretation of the geometrical dimensions, volume, color, and structure of the TLE. When a TLE is detected, the gondola will be pointed accurately in order to have the atmosphere where the identify TLE just occurs in the center of the imager detector and the acquisition of hyperspectral cubes of data will start with an acquisition rate in the range of 5–60 cubes/min. The whole measurement and calibration strategy will be driven by a PC board. The steps of this strategy are described in Table I. The first step in the study was to evaluate the feasibility of hyperspectral detection of the TLE signatures and to determine the technical setup of the one or two hyperspectral imagers that should be included in the gondola. Our decision to focus initially on blue jets is based on several considerations. Among the different TLEs, only blue jets and TGF occur in the lower stratosphere, i.e., reachable by a stratospheric balloon. We are better informed about blue jets, as they have been more frequently observed and characterized than TGF. In addition, as described in Section III, both fundamental and hot band signatures can be observed for blue jets. This investigation into blue jets will enable us to assess the ability of the instrumentation to measure their chemical impact and establish whether locally such discharges can have an impact

TABLE I
MEASUREMENT STRATEGY

| Step | Name | Description |
|---|---|---|
| 0 | Waiting for the next thunderstorm | Pointing of the gondola in the thunderstorm direction once activity is detected. |
| 1 | TLE detection | Calibration of the hyperspectral imager and panchromatic camera startup for TLE detection. Pointing of the hyperspectral imager FOV on the TLE direction once an event is detected. |
| 2 | Monitoring | Record of hyperspectral data-cubes. After a few minutes, return to step 1) or go to step 3) or 4). |
| 3 | End of acquisition | Return to step 0). |
| 4 | End of the experiment | End of the flight. |

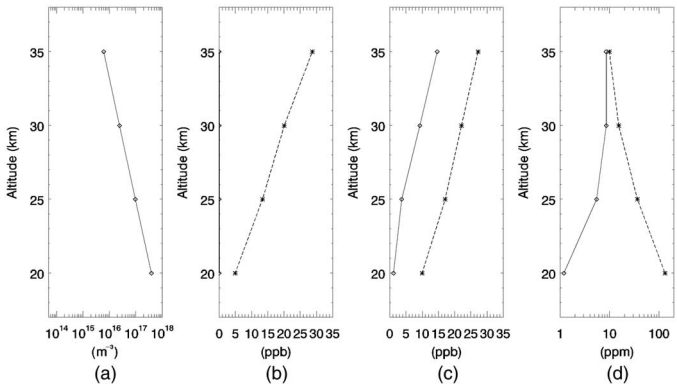


Fig. 2. (a) Vertical profiles of electron concentration associated with the blue jet event. (b)–(d) Vertical profiles of NO, $NO_2$, and $O_3$ mixing ratios. The solid line corresponds to initialization before the blue jet event observed by [43] on July 22, 2007 at $23°28'$N–$120°52'$E at 12:00 UTC, and the dotted lines after, respectively, 0.8, 275, and 30 s for NO, $NO_2$, and $O_3$ of MIPLASMO simulations. These durations correspond to the maximum production for each species.

on the ozone layer in the stratosphere, which is very sensitive to NOx content. The rate at which blue jets and gigantic jets occur is currently not well known, more and more measurements from the ground have been done recently [41]–[43]. This blue jet study is a first step and we will continue the study to evaluate the capability of the instrumentation to measure the impact of sprites and halos.

## III. EXPECTED INFRA-RED SIGNATURES OF A SINGLE BLUE JET ATMOSPHERIC PERTURBATION

To assess the feasibility of HALESIS, it was necessary to perform an estimation of TLEs infrared signatures to be compared with available IR hyperspectral instrumentation technical specifications. It is important to point out that the aim of this feasibility study was not to establish an exhaustive description of the phenomena but to provide an order of magnitude of the signature intensities in order to verify if they are measurable. To achieve this, we need first to have an order of magnitude of the chemical species produced by an electrical discharge in the stratosphere as a function of altitude. It is then possible to estimate the infrared radiometric signature assuming a simple geometrical representation of the blue jet.

### *A. Estimation of Blue Jet Perturbation on Stratospheric Composition*

To determine the order of magnitude of the chemical perturbation induced by a blue jet discharge, we evaluated the production of $NO_x$ and $O_3$ using the stratospheric chemical model MIPLASMO [44]. This model was developed to interpret chemical measurements from several stratospheric balloon-borne instruments during the last decade. It has been used in particular to investigate processes associated with polar stratospheric clouds, nitrogen oxides and chlorine activation [45]–[49]. In its box version, the model can predict the time evolution of 30 chemical species associated with the full stratospheric $O_3$ chemistry (nitrogen, chlorine, and bromine families). Recently, new developments have been made to include in a one-dimensional version (from 15 to 40 km) the specific chemistry due to electric discharge according to the simplified chemical scheme from Mishin [14].

This scheme uses the electric field and the electron concentration to calculate reaction rates. These two parameters were calculated using a discharge propagation code based on the studies by Raizer *et al.* [50], [51]. This code considers a blue jet as a streamer initiated by a bidirectional leader discharge, emerging from the anvil and sustained by a moderate cloud charge. The streamer growth depends on the electrical field induced by the initial cloud charge and the initial altitude. We consider a charge of $20°$C in a sphere with a radius of 3 km (the part of the clouds which is charged) corresponding to a potential of 60 000 kV at 15 km. The starting altitude of the leader is then 15 km and it propagates up to 50 km. Fig. 2(a) presents the electron concentration produced as a function of altitude according to Pasko *et al.* [27].

To describe the chemistry associated with the blue jet discharge, 37 chemical reactions and 8 chemical species (related to excited species and ions) were included in the MIPLASMO model (see Mishin [14] for a detailed list). To prevent numerical instabilities, the time step of the model was progressively reduced from 30 s (ozone chemical time step) to $0.1$ μs during 0.1 ms when the blue jet appears (electric chemical time step), then a time step of 0.1 ms was used during 0.1 s, next the time step of 0.1 s was used up to 10 s, and finally the ozone chemical time step was again applied.

Initial mixing ratio vertical profiles of the chemical species come from the outputs of the REPROBUS CTM model [52] widely used for stratospheric chemical studies. These profiles correspond to the chemical background conditions on July 22, 2007 at $23°28'$N and $120°52'$E at 12:00 UTC when a blue jet event was observed [43].

Volume mixing ratios of NO, $NO_2$, and $O_3$ before the blue jet and after the discharge are presented in Fig. 2(b)–(d). Because the chemical impact of the discharge is time and species dependent, we choose to present the maximum values obtained for each species, i.e., after 0.8, 275, and 30 s for NO, $NO_2$, and $O_3$, respectively. NO production increases as a function of altitude with more than 30 ppbv at 35 km. The production of $NO_2$ is roughly 10 ppbv whatever the altitude considered. $O_3$ production is maximum at 20 km with a very strong value, but this production is directly linked to the number of electrons at the top of the streamer calculated using Pasko *et al.* (at $20\,\mathrm{km}$ $10^{17}\ \mathrm{m}^{-3}$ electrons) [27].

Mishin reports a lower $O_3$ production at 20 km but they consider only a $10^{13}\ \mathrm{m}^{-3}$ electron concentration [14]. In addition, this production is very local (top of the streamer) without considering any information about the spatial extent/shape of the streamer and atmospheric diffusion process. The chemical species are not at chemical equilibrium with the environment, and those results correspond to the local enhancement due to the discharge.

### *B. Fundamental Band Infrared Signatures*

Theoretical predictions were then used to provide an estimation of a blue jet infrared radiometric signature using the line by line radiative transfer model (LBLRTM) [53], [54]. This line by line model was chosen due to the possibility of taking into account the non-LTE (NLTE) hypothesis (see Section III-C). Simulations were done considering a limb line of sight from a stratospheric balloon for several tangent heights and an elevation of the line of sight of $0°$. The atmosphere was discretized into concentric layers each 1 km thick. When considering the blue jet perturbation, some additional layers were added so that a disturbed area located at about 50 km from the observer is crossed by the line of sight. The length of the pathway in the disturbed area is, respectively, 4.0, 5.3, 6.6, and 7.9 km for an observer flying at a tangent height $h_i$ (i = 1 to 4), respectively, of 20, 25, 30, and 35. In a first step, background atmosphere radiances were generated with a spectral resolution of $2\,\mathrm{cm}^{-1}$ using the U.S. standard description of atmosphere [55] for each layer. In a second step, perturbed spectral radiances were calculated (with the same spectral resolution): the concentrations of NO, $NO_2$, $O_3$, and $NO^+$ were initialized with theoretical predictions inside the perturbed layers (where the concentration of those species was considered homogeneous). Thus, our simulation is equivalent to a standard atmosphere in which we inserted a conical perturbed region with a full angle of $15°$ and a base width of 4 km at an altitude of 20.2 km. Values of the perturbed concentrations were selected at the time when they reached their highest value and are presented in Fig. 2.

Calculations were done successively for the four values of $h_i$. Two spectral ranges (TIR and MIR) were covered depending on the molecule studied. The results are presented in Fig. 3(a) (MIR range) and 3(b) (TIR range). Background atmospheric radiances are plotted on the top row of Fig. 3(a) and (b). The difference between the perturbed and background spectral radiances is presented on the bottom row of Fig. 3(a) and (b). The positions of the spectral signatures of $O_3$, NO, and $NO_2$ are indicated in the figure. Then, the calculation was repeated for increasing values of spectral resolution from 0.1 to $20\,\mathrm{cm}^{-1}$ in order to evaluate the dependence of the intensity of the signature versus the spectral resolution. To determine the required instrumental sensitivity, we have plotted the maximum difference between a background spectrum and a perturbed spectrum versus the wavelength for $O_3$, NO, $NO_2$, and $NO^+$ (Fig. 4). This difference represents the typical instrumental sensitivity level that should be reached to detect such signatures with a signal-to-noise ratio (S/N) of one. It is important to note that the predicted signatures were obtained assuming a simplified geometric scheme, and that they have at least one order of magnitude of uncertainty. When the spectral resolution is degraded (i.e., when the width of the apparatus function increases) the intensity of the disturbance spectrum decreases while the acquisition rate can be increased. That explains why the detection limit of the instrument is higher for lower spectral resolutions at a given integration time (e.g., possibility to perform spectra co-addition and decrease instrumental noise). While the predicted enhancement of $O_3$ concentration is clearly detectable by hyperspectral imagery in both the TIR and MIR spectral range, the sensitivity levels required to monitor $NO_2$, and further to monitor NO in the MIR range, are very low. For the $O_3$ local disturbance, signatures are intense enough to be very easily detectable up to 30 km in the TIR range [Fig. 3(b); 20, 30, and 35 km]. In the MIR range, the $O_3$ signature also decreases from 20 to 35 km, whereas the signatures of $NO_2$ and NO are expected to remain constant based on the altitude. But the NO signature—which is very low and could be hardly detected—is hidden by the $O_3$ signature up to 25 km [Fig. 3(a); 20, 30, and 35 km]. To compare the signature intensities with the detection limit of a typical spectro-imager, the dashed line and dotted line plotted in Fig. 4, respectively, indicate the best detection limit of a panel of commercial FTIR-based hyperspectral imagers, and multipixel imagers. Hyperspectral imagers correspond to a reduced $32 \times 32$ pixel window whereas the maximum size of multipixel sensor windows is $8 \times 8$ pixels. A 10-s equivalent integration time was used. We can see in Fig. 4 that a typical commercially available hyperspectral imager, like a scientific research prototype, could be used to easily detect the $O_3$ disturbance signature at low altitude in the TIR range. However, as multipixel imagers can reach lower detection limits, they are more promising for the purposes of HALESIS. But the price to pay is then the poor spatial resolution. A typical spectral resolution should be fixed in the range from 5 to $15\,\mathrm{cm}^{-1}$. Indeed, selecting a lower spectral resolution would imply too low an acquisition frequency, while a higher acquisition frequency would result in a decrease of the selectivity of the measurements. Even if the MIR spectral range contains the fundamental bands of interesting species (like NO, $NO_2$, and $NO^+$), the detection of such signatures will require using a low spectral resolution and an integration time as high as possible (typically 10 s). Data processing (e.g., co-averaging, spatial, and spectral binning) should improve instrumental sensitivity, making it possible to detect $NO_2$ and NO. In the spectral range from 2200 to $2400\,\mathrm{cm}^{-1}$ the spectrum is saturated due to $CO_2$ absorption, so that it is impossible to detect $NO^+$ in this spectral range and the results for this species are not presented here.

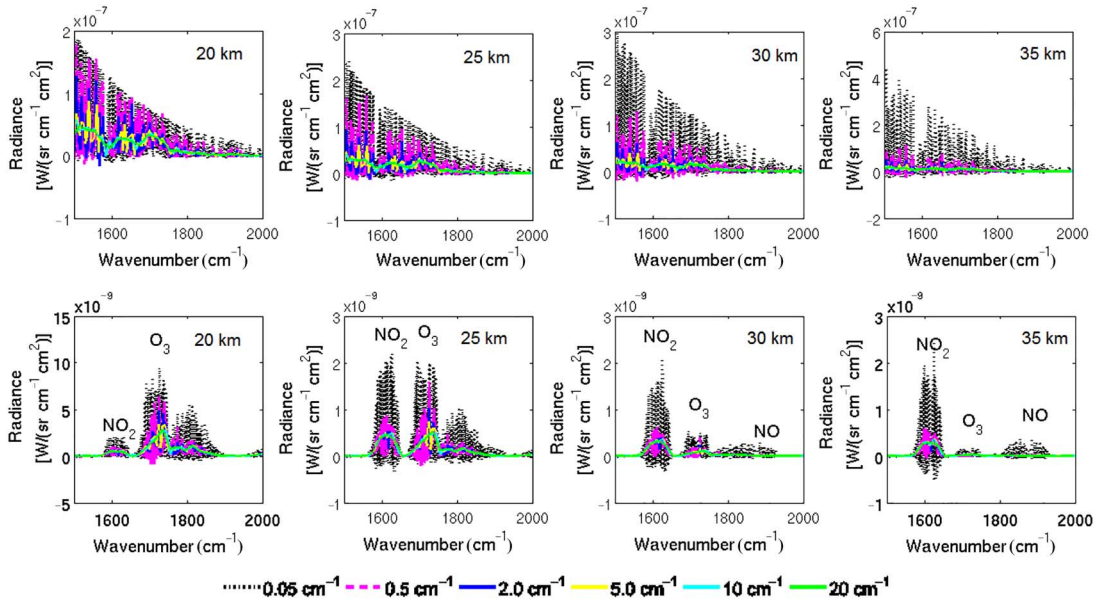


(a)

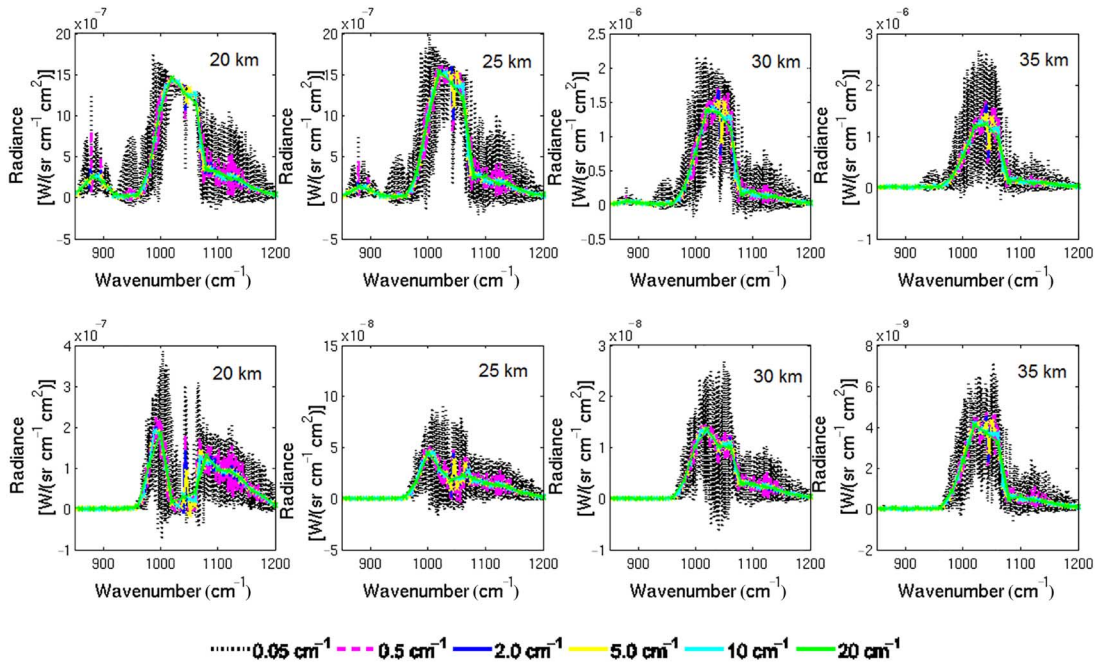


(b)

Fig. 3. (a) Background radiance (top) and blue jet signatures, i.e., difference between perturbed and background radiances (bottom) for four different altitudes, and six different spectral resolutions in the MIR spectral range. (b) Background radiance (top) and blue jet signatures, i.e., difference between perturbed and background radiances (bottom) for four different altitudes and six different spectral resolutions in the TIR spectral range.

### C. Hot Band Infrared Signatures

Energy deposition following a TLE event produces molecules in vibrationally excited levels. The LTE is perturbed, which means an NLTE situation, and it is then necessary to consider the population of each vibrational energy level individually in order to simulate the accurate radiative transfer of hot bands. Taking the NLTE hypothesis into account does not significantly change the fundamental band signature, but some spectral signatures in the hot vibrational bands can appear with significantly larger amplitudes than for the fundamental ones. The interest of this second part of the study is twofold. First, the infrared signatures of hot bands are more intense, the required sensitivity level to detect them is higher and the technical feasibility can be more easily reached. Secondly, if such signatures are detectable, it will be possible to monitor the vibrational chemistry induced by TLEs (i.e., the chemistry that considers

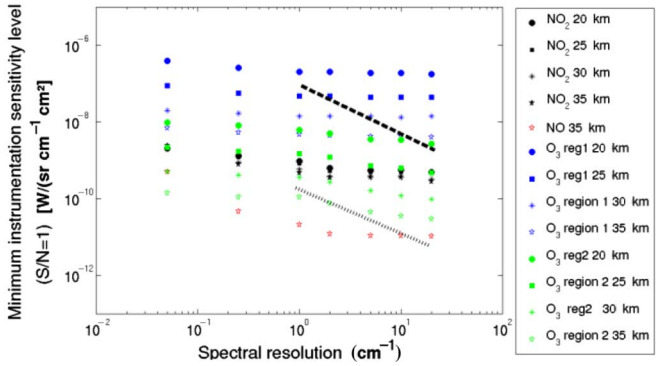


Fig. 4. Required instrumental sensitivity to detect an infrared signature with an S/N of 1 for different species and altitudes. The dashed line and the dotted line, respectively, indicate the best detection limit of a panel of FTIR-based commercially available hyperspectral imagers and multipixel imagers.

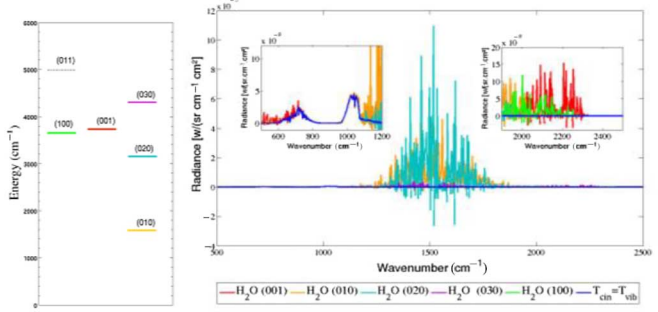


Fig. 5. Vibrational energy levels (left) and individual signatures (right) for a 400-K increase of a vibrational temperature in the perturbed region for an observer at 35 km and a limb line of sight.

each vibrational state of a molecule as an individual species) so that our experiment will provide important complementary information concerning the energy deposition.

The aim of this part of the study is to give an estimation of the hot band infrared signatures due to the perturbation of the molecular vibrational temperature by a single blue jet. It is important to recall here that this work is a sensitivity study. To take into account the NLTE hypothesis—to consider the population of each energy level individually—the same theoretical predictions and the same geometry assumptions as for the fundamental band study were used (see Section III-B). The study was performed for all the vibrational levels available in LBLRTM under NLTE mode (version 12.1—see http://rtweb.aer.com/lblrtm.html for more information). When a molecular species was predicted to have an unaffected concentration (e.g., $CO_2$), its concentration was left at its background value, and only the corresponding vibrational level populations were affected. When all the vibrational temperatures $T_{vib}^{mol}(l)$ for all the available vibrational levels $l$ of all the studied molecules $mol$ are equal to the kinetic temperature $T_{kin}$, the case is equivalent to the LTE case. Then the vibrational levels were successively populated. Simulations for $H_2O$ are shown in Fig. 5. For this molecule, no disturbance in concentration was predicted and calculations for the first six vibrational levels are accessible with LBLRTM [Fig. 5(a)]. A temperature increment $\Delta T_{vib}$ was added successively for each

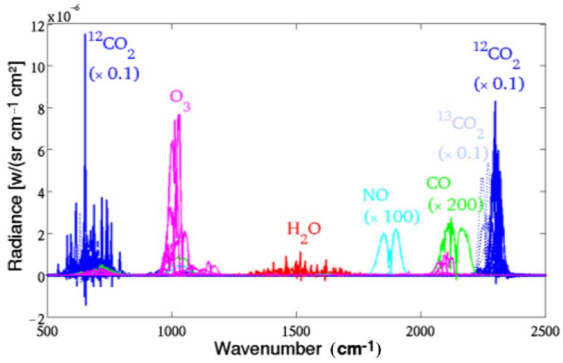


Fig. 6. Identification of the main NLTE signatures for a 400-K increase of individual vibrational temperatures in the perturbed region for an observer at 35 km and a limb line of sight. All the vibrational signatures corresponding to the same species are plotted in the same color. For reasons of clarity, $^{12}CO_2$, NO, and CO have been scaled, respectively, with a factor of 0.1, 100, and 200.

vibrational level to quantify the impact of the corresponding population level perturbation on the radiance spectra

$$T_{vib}^{mol}(l) = T_{kin} + \Delta T_{vib}. \tag{1}$$

The signature due to the perturbation of the first six levels of $H_2O$ is presented in Fig. 5(b). Note that there is substantial overlap between the signatures due to a perturbation of the different vibrational levels. While the first scientific flight will be dedicated to identifying the main detectable signatures using a low level of resolution, a second flight will be required to explore some selected small spectral windows with a higher resolution level. This would be useful to distinguish between the different signatures and monitor the vibrational chemistry associated with TLE occurrences. The study was repeated for other chemical species. It allowed identification of the most intense individual spectral signatures corresponding to an increase in each vibrational level population, considering a spectral resolution of $3\,\mathrm{cm}^{-1}$ (Fig. 6). The same conclusion as for the fundamental band can be deduced concerning the TIR range: ozone signatures should be easily observed from this spectral range with a spectral resolution that should be set in the range from 5 to $10\,\mathrm{cm}^{-1}$. This would provide both a good selectivity between the different vibrational signatures and a sufficient sensitivity. In the MIR spectral range, the hot band signature should appear with a higher intensity than that of the fundamental bands. In particular, the $1800 - 2500\,\mathrm{cm}^{-1}$ spectral range is the most suitable to detect the TLE effect on the $CO_2$ vibrational temperature: signatures are quite as intense as in the $500 - 800\,\mathrm{cm}^{-1}$ spectral range. Finally the sensitivity versus the increment of vibrational temperature $\Delta T_{vib}$ was evaluated for all the vibrational levels considered for a given species (Fig. 7). For each molecular species, the temperature increment effect for values successively of 10, 100, 200, and 400 K was considered. For a given molecule, all the energy levels were disrupted simultaneously. In this case, the most intense hot band signatures define the pattern. The instrument sensitivity level to detect the signatures with an S/N equal to 1 is plotted versus the perturbation amplitude $\Delta T_{vib}$ and compared with the best hyperspectral detection levels.

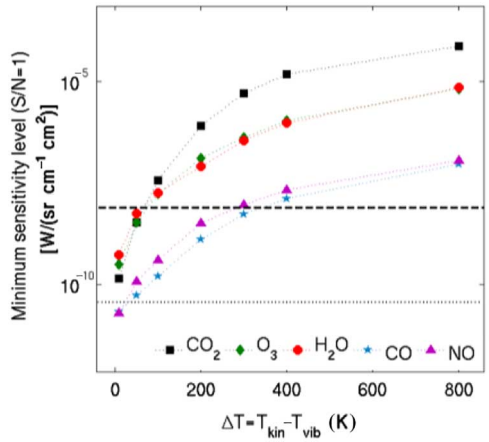


Fig. 7. Required sensitivity level to detect the spectral signature with an $S/N = 1$ versus the simultaneous increase of all the available vibrational temperatures of the molecule, for an observer at 35 km and a limb line of sight.

## IV. Summary

The effect of TLEs on the atmospheric composition is an open and important question. Although several theoretical and experimental studies have attempted to answer it, the lack of suitable experimental data is a shortcoming that hampers our understanding of the physics and chemistry induced by these effects. We are preparing an experiment to measure the atmospheric perturbation in the minutes following a TLE from a stratospheric balloon flying at an altitude from 20 to 35 km. To assess the feasibility of the experiment, we have simulated the spectral perturbation induced by an isolated blue jet, taking into account theoretical predictions. Under the selected assumptions, this study has established the feasibility and the interest of detecting the local enhancement of $O_3$, maybe $NO_2$, and with greater difficulty, NO that could be produced by a single blue jet at low altitude (typically 20–35 km). At higher altitudes (typically above 35 km), spectral signatures in the hot vibrational bands appear with larger amplitudes than for the fundamental ones. The NLTE signature induced by a blue jet will be probably detectable both in the TIR ($O_3$) range and in the MIR range ($CO_2$, $H_2O$, CO, NO, etc.). Moreover, NLTE detection will provide complementary information about the energy deposition and the vibrational chemistry caused by TLEs.

Our study clearly demonstrates the interest of continuing to study the chemistry induced by vibrational excitation from TLEs. The signature of hot bands is much more intense than that of fundamental bands, and it may be possible to detect the perturbation induced in NO and CO spectral signatures at 35 km if the NLTE effect is sufficient. The selected resolution of $3\,\mathrm{cm}^{-1}$ will unambiguously distinguish the signatures of different species but a second mission will probably be required if hot band signatures are detected during the first balloon flights. In this case, an improved spectral resolution ($1\,\mathrm{cm}^{-1}$ or better) in selected spectral windows would be necessary in order to distinguish the different vibrational level disturbance signatures. Lastly, if signatures due to the perturbation of some vibrational levels cannot be distinguished individually, it may be necessary to perform a second set of measurement campaigns with instrumentation with higher spectral resolution in spectral regions identified from the data recorded during the first measurement campaigns.

In summary, we conclude that, to detect the radiance perturbation induced by a TLE, it is necessary to use an instrument with high capacities in terms of sensitivity and acquisition frequency. Commercially available instruments already exist to perform such measurements but their capacities are often close to the required performances. The main limitations of FTIR spectro-imagers are the strong correlation between the window size, the spectral resolution, the acquisition frequency, and the sensitivity level. While the technique is perfectly suited for the aim of HALESIS in the TIR spectral range, things become more difficult in the MIR range where, except for the detection of $CO_2$ hot bands, the experiment requires both a fast and sensitive detection. However, innovative instrumental approaches exist and open up new avenues for the experiment [37]–[39], [56]–[58].

## Acknowledgment

The authors would like to thank CSTB (Comité Scientifique et Technique Ballon) of CNES (French space agency) for the financial support to perform the feasibility study. They also thank C. Camy-Peyret (IPSL) who initiated this research project, supplied scientific and technical recommendations, and for fruitful discussions.

## References

[1] R. Franz, R. Nemzek, and J. Winckler, "Television image of a large upward electrical discharge above a thunderstorm system," *Science*, vol. 249, no. 4964, pp. 48–51, 1990.

[2] G. J. Fishman *et al.*, Discovery of intense gamma-ray flashes of atmospheric origin. *Sci.*, vol. 264, no. 5163, pp. 1313–1316, 1994.

[3] J. Chern *et al.*, "Global survey of upper atmospheric transient luminous events on the ROCSAT-2 satellite," *J. Atmos. Sol. Terr. Phys.*, vol. 65, no. 5, pp. 647–659, 2003.

[4] A. B. Chen *et al.*, "Global distributions and occurrence rates of transient luminous events," *J. Geophys. Res. Space Phys.*, vol. 113, no. A8, p. A08306, 2008.

[5] S. B. Mende *et al.*, "Spacecraft based studies of transient luminous events," in *Sprites, Elves and Intense Lightning Discharges*. New York, NY, USA: Springer, 2006, pp. 123–149.

[6] E. M. Wescott, D. Sentman, D. Osborne, D. Hampton, and M. Heavner, "Preliminary results from the Sprites94 aircraft campaign: 2. Blue jets," *Geophys. Res. Lett.*, vol. 22, no. 10, pp. 1209–1212, 1995.

[7] P. Israelevich *et al.*, "Transient airglow enhancements observed from the space shuttle Columbia during the MEIDEX sprite campaign," *Geophys. Res. Lett.*, vol. 31, no. 6, p. L06124, 2004.

[8] V. P. Pasko, M. A. Stanley, J. D. Mathews, U. S. Inan, and T. G. Wood, "Electrical discharge from a thundercloud top to the lower ionosphere," *Nature*, vol. 416, no. 6877, pp. 152–154, 2002.

[9] E. A. Mareev, M. Füllekrug, E. A. Mareev, and M. J. Rycroft, *Sprites, Elves and Intense Lightning Discharges*, vol. 225. New York, NY, USA: Springer, 2006.

[10] V. P. Pasko, Y. Yair, and C.-L. Kuo, "Lightning related transient luminous events at high altitude in the earth's atmosphere: Phenomenology, mechanisms and effects," *Space Sci. Rev.*, vol. 168, no. 1–4, pp. 475–516, 2012.

[11] V. Surkov and M. Hayakawa, "Underlying mechanisms of transient luminous events: A review," *Ann. Geophys.*, vol. 30, no. 8, pp. 1152–1212, 2012.

[12] E. Wescott *et al.*, "New evidence for the brightness and ionization of blue starters and blue jets," *J. Geophys. Res. Space Phys.*, vol. 106, no. A10, pp. 21549–21554, 2001.

[13] V. P. Pasko and J. J. George, "Three-dimensional modeling of blue jets and blue starters," *J. Geophys. Res. Space Phys.*, vol. 107, no. A12, pp. SIA 12-1–SIA 12-16, 2002.

[14] E. Mishin, "Ozone layer perturbation by a single blue jet," *Geophys. Res. Lett.*, vol. 24, no. 15, pp. 1919–1922, 1997.
[15] N. Liu and V. P. Pasko, "Modeling studies of NO-$\gamma$ emissions of sprites," *Geophys. Res. Lett.*, vol. 34, no. 16, p. L16103, 2007.
[16] F. J. Gordillo-Vázquez, "Air plasma kinetics under the influence of sprites," *J. Phys. Appl. Phys.*, vol. 41, no. 23, p. 234016, 2008.
[17] C.-F. Enell *et al.*, "Parameterisation of the chemical effect of sprites in the middle atmosphere," *Ann. Geophys.*, no. 28, pp. 13–27, 2008.
[18] P. R. Krehbiel *et al.*, "Upward electrical discharges from thunderstorms," *Nat. Geosci.*, vol. 1, no. 4, pp. 233–237, 2008.
[19] Y. Hiraki, Y. Kasai, and H. Fukunishi, "Chemistry of sprite discharges through ion-neutral reactions," *Atmos. Chem. Phys.*, vol. 8, no. 14, pp. 3919–3928, 2008.
[20] E. Blanc, F. Lefeuvre, R. Roussel-Dupré, and J. Sauvaud, "TARANIS: A microsatellite project dedicated to the study of impulsive transfers of energy between the earth atmosphere, the ionosphere, and the magnetosphere," *Adv. Space Res.*, vol. 40, no. 8, pp. 1268–1275, 2007.
[21] T. Neubert *et al.*, "The atmosphere–space interactions monitor (ASIM) for the international space station," in *Proc. Int. Living Star Workshop (ILWS)*, 2006, pp. 19–20.
[22] S. Beirle, U. Platt, M. Wenig, and T. Wagner, "NOx production by lightning estimated with GOME," *Adv. Space Res.*, vol. 34, no. 4, pp. 793–797, 2004.
[23] S. Beirle, H. Huntrieser, and T. Wagner, "Direct satellite observation of lightning-produced NOx," *Atmos. Chem. Phys.*, vol. 10, no. 22, pp. 10965–10986, Nov. 2010.
[24] E. J. Bucsela *et al.*, "Lightning-generated NOx seen by the ozone monitoring instrument during NASA's tropical composition, cloud and climate coupling experiment (TC4)," *J. Geophys. Res. Atmos.*, vol. 115, no. D10, p. D00J10, May 2010.
[25] H. Huntrieser *et al.*, "Airborne measurements of NOx, tracer species, and small particles during the European lightning nitrogen oxides experiment," *J. Geophys. Res. Atmos.*, vol. 107, no. D11, p. ACH 5-1, Jun. 2002.
[26] M. J. Rycroft, S. Israelsson, and C. Price, "The global atmospheric electric circuit, solar activity and climate change," *J. Atmos. Sol. Terr. Phys.*, vol. 62, no. 17–18, pp. 1563–1576, Nov. 2000.
[27] V. P. Pasko, "Theoretical modeling of sprites and jets," in *Sprites, Elves and Intense Lightning Discharges*. New York, NY, USA: Springer, 2006, pp. 253–311.
[28] H. Peterson, M. Bailey, J. Hallett, and W. Beasley, "NOx production in laboratory discharges simulating blue jets and red sprites," *J. Geophys. Res. Space Phys.*, vol. 114, no. A12, p. A00E07, 2009.
[29] J. de Urquijo and F. Gordillo-Vazquez, "Comment on "NOx production in laboratory discharges simulating blue jets and red sprites" by Harold Peterson et al.," *J Geophys. Res.*, vol. 115, no. A12, p. A12319, 2010.
[30] S. Nijdam, E. van Veldhuizen, and U. Ebert, "Comment on "NOx production in laboratory discharges simulating blue jets and red sprites" by H. Peterson et al.," *J. Geophys. Res. Space Phys.*, vol. 115, no. A12, p. A12305, 2010.
[31] H. Peterson, M. Bailey, J. Hallett, and W. Beasley, "Reply to comment by J. de Urquijo and FJ Gordillo-Vázquez on "NOx production in laboratory discharges simulating blue jets and red sprites"," *J. Geophys. Res. Space Phys.*, vol. 115, no. A12, p. A12320, 2010.
[32] H. Peterson, M. Bailey, J. Hallett, and W. Beasley, "Reply to comment by S. Nijdam et al. on "NOx production in laboratory discharges simulating blue jets and red sprites"," *J. Geophys. Res. Space Phys.*, vol. 115, no. A12, p. A12306, 2010.
[33] C. J. Rodger, A. Seppälä, and M. A. Clilverd, "Significance of transient luminous events to neutral chemistry: Experimental measurements," *Geophys. Res. Lett.*, vol. 35, no. 7, p. L07803, 2008.
[34] E. Arnone *et al.*, "Seeking sprite-induced signatures in remotely sensed middle atmosphere $NO_2$," *Geophys. Res. Lett.*, vol. 35, no. 5, p. L05807, 2008.
[35] M. Endemann, "MIPAS instrument concept and performance," in *Proc. Eur. Symp. Atmos. Meas. Space*, Noordwijk, The Netherlands, 1999, pp. 18–22.
[36] E. Arnone *et al.*, "Seeking sprite-induced signatures in remotely sensed middle atmosphere $NO_2$: Latitude and time variations," *Plasma Sources Sci. Technol.*, vol. 18, no. 3, p. 034014, 2009.
[37] J. Ungermann *et al.*, "Towards a 3-D tomographic retrieval for the air-borne limb-imager GLORIA," *Atmos. Meas. Tech.*, vol. 3, no. 6, pp. 1647–1665, 2010.
[38] L. Rousset-Rouviere *et al.*, "Sysiphe, an airborne hyperspectral imaging system for the VNIR-SWIR-MWIR-LWIR region," in *Proc. 7th EARSeL Workshop Imag. Spectrosc.*, 2011, pp. 1–12.
[39] L. Rousset-Rouviere *et al.*, "SYSIPHE: The new-generation airborne remote sensing system," *Proc. SPIE*, p. 853202, 2012.
[40] J.-B. Renard *et al.*, "SALOMON: A new, light balloonborne UV-visible spectrometer for nighttime observations of stratospheric trace-gas species," *Appl. Opt.*, vol. 39, no. 3, pp. 386–392, 2000.
[41] O. A. van der Velde *et al.*, "Multi-instrumental observations of a positive gigantic jet produced by a winter thunderstorm in Europe," *J. Geophys. Res. Atmos.*, vol. 115, no. D24, p. D24301, 2010.
[42] S. Soula *et al.*, "Gigantic jets produced by an isolated tropical thunderstorm near Réunion Island," *J. Geophys. Res. Atmos.*, vol. 116, no. D19, p. D19103, Oct. 2011.
[43] J. K. Chou *et al.*, "Optical emissions and behaviors of the blue starters, blue jets, and gigantic jets observed in the Taiwan transient luminous event ground campaign," *J. Geophys. Res. Space Phys.*, vol. 116, no. A7, p. A07301, Jul. 2011.
[44] E. Riviere *et al.*, "Role of lee waves in the formation of solid polar stratospheric clouds: Case studies from February 1997," *J. Geophys. Res. Atmos.*, vol. 105, no. D5, pp. 6845–6853, 2000.
[45] J.-B. Renard *et al.*, "Measurements and simulation of stratospheric NO3 at mid and high latitudes in the northern hemisphere," *J. Geophys. Res. Atmos.*, vol. 106, no. D23, pp. 32387–32399, Dec. 2001.
[46] E. D. Rivière *et al.*, "On the interaction between nitrogen and halogen species in the Arctic polar vortex during THESEO and THESEO 2000," *J. Geophys. Res. Atmos.*, vol. 107, no. D5, p. 8311, Mar. 2002.
[47] E. D. Rivière, Y. Terao, and H. Nakajima, "A Lagrangian method to study stratospheric nitric acid variations in the polar regions as measured by the improved limb atmospheric spectrometer," *J. Geophys. Res. Atmos.*, vol. 108, no. D23, p. 4718, 2003.
[48] C. Brogniez *et al.*, "Polar stratospheric cloud microphysical properties measured by the microRADIBAL instrument on 25 January 2000 above Esrange and modeling interpretation," *J. Geophys. Res. Atmos.*, vol. 108, no. D6, p. 8332, Mar. 2003.
[49] A. Grossel *et al.*, "In situ balloon-borne measurements of HNO3 and HCl stratospheric vertical profiles influenced by polar stratospheric cloud formation during the 2005–2006 Arctic winter," *J. Geophys. Res. Atmos.*, vol. 115, no. D21, p. D21303, Nov. 2010.
[50] Y. P. Raizer, G. M. Milikh, and M. N. Shneider, "On the mechanism of blue jet formation and propagation," *Geophys. Res. Lett.*, vol. 33, no. 23, p. L23801, Dec. 2006.
[51] Y. P. Raizer, G. M. Milikh, and M. N. Shneider, "Leader–streamers nature of blue jets," *J. Atmos. Sol. Terr. Phys.*, vol. 69, no. 8, pp. 925–938, Jun. 2007.
[52] F. Lefevre, G. Brasseur, I. Folkins, A. Smith, and P. Simon, "Chemistry of the 1991–1992 stratospheric winter: Three-dimensional model simulations," *J. Geophys. Res. Atmos.*, vol. 99, no. D4, pp. 8183–8195, 1994.
[53] S. A. Clough, M. J. Iacono, and J. Moncet, "Line-by-line calculations of atmospheric fluxes and cooling rates: Application to water vapor," *J. Geophys. Res. Atmos.*, vol. 97, no. D14, pp. 15761–15785, 1992.
[54] S. Clough *et al.*, "Atmospheric radiative transfer modeling: A summary of the AER codes," *J. Quant. Spectrosc. Radiat. Transfer*, vol. 91, no. 2, pp. 233–244, 2005.
[55] U. Coesa, "Standard Atmosphere, 1976," *US Gov. Print. Off. Wash. DC*, 1976.
[56] Y. Ferrec *et al.*, "Experimental results from an airborne static Fourier transform imaging spectrometer," *Appl. Opt.*, vol. 50, no. 30, pp. 5894–5904, 2011.
[57] N. Guérineau *et al.*, "Compact designs of hyper-or multispectral imagers compatible with the detector dewar," *Proc. SPIE*, p. 801229, 2011.
[58] H. Oelhaf, P. Preusse, and F. Friedl-Vallon, "GLORIA: A new instrument for atmospheric research deployed to Geophysica and HALO during the ESSENCE and TACTS/ESMVAL missions," in *Proc. EGU Gen. Assem. Conf. Abstr.*, 2013, vol. 15, p. 10008.

**Laurence Croizé** received the Magistère Inter-Universitaire de Physique from École Normale Supérieure of Paris, Paris, France, in 2005, and the Ph.D. degree in molecular spectroscopy from the University of Pierre and Marie Curie, Paris, France, in 2008.

From 2008 to 2014, she was a Postdoctoral Researcher with French Alternative Energies and Atomic Energy Commission (Commissariat à l'énergie atomique et aux énergies alternatives), Saclay, France, then with Université du Littoral Côte d'Opale, Dunkirk, France, and last with Laboratoire Atmosphère Millieux Oberservations spatiales (LATMOS). Since 2014, she has been a Research Scientist with French Aerospace Laboratory (ONERA), Palaiseau, France. Her research interests include absorption spectroscopy for laboratory experiment and for atmospheric studies, instrumentation (spectrometry and hyperspectral imagery), and radiative transfer.

**Sébastien Payan** received the M.Sc. degree in experimental physics from the University of Reims, Reims, France, in 1993, and the Ph.D. degree in molecular physics and geoscience from the University of Pierre and Marie Curie, Paris, France, in 1996.

From 1996 to 1999, he worked as a Research Assistant with Laboratoire de Physique Moléculaire and Applications (LPMA) with a founding by the French Space Agency, CNES, and the French Scientific Research Center, CNRS. From 1999 to 2011, he was an Assistant Professor with the Department of Physics, University of Pierre and Marie Curie. Since 2011, he has been a Full Time Professor with the physics and the geosciences departments. His research interests include instrumental and theoretical fields related to atmospheric composition from hyperspectral imagery to urban *in situ* measurements.

**Jérôme Bureau** received the Engineer Diploma in physics from the Institut National Polytechnique de Grenoble, Grenoble, France, the M.S. degree in materials science from the University of Joseph Fourier, Grenoble, France, in 1997, and the Ph.D. degree in physics from the University of Paris 6, Paris, France, in 2009.

From 2002 to 2004, he was as an Engineer with the Laboratoire de Meteorologie Dynamique, Palaiseau, France. From 2004 to 2012, he was an Engineer with the Laboratoire de Physique Moleculaire pour l'Atmosphere et l'Astrophysique, Paris, France, and with Noveltis Company, Toulouse, France (2008–2009). From 2013, he was a Research Engineer with the Laboratoire Atmosphères, Milieux, Observations Spatiales, Paris, France. His research interests include radiative transfer and infrared spectroscopy.

**Fabrice Duruisseau** received the B.S. and M.S. degrees in physics from the University of Orléans, Orléans, France, in 2011. He is currently pursuing the Ph.D. degree in atmospheric physics from the Laboratoire de Physique et chimie de l'Environnement et de l'Espace (LPC2E), Orléans, France.

His research interests include the stratospheric dynamic, the atmospheric electrical activities (TLEs), the modeling of the atmospheric dynamic, the atmospheric measurements, the study of the balloon trajectories, and their behavior in the high stratosphere.

**Rémi Thiéblemont** was born in Paris, in 1986. He received the M.S. degree in atmospheric and space plasma physics and the Ph.D. degree in atmospheric sciences from the University of Orléans, Orléans, France, in 2009 and 2012, respectively.

Since 2013, he has been working as a Postdoctoral Researcher with GEOMAR Helmholtz Center for Ocean Research. His research interests include stratosphere dynamics and chemistry, natural climate variability, and sun/climate connections.

**Nathalie Huret** received the M.Sc. degree in physics from the University Blaise Pascal, Clermont-Ferrand, France, in 1990, and the Ph.D. degree in Atmospheric Physics from the University Blaise Pascal, Clermont-Ferrand, France, in 1994.

From 1994 to 2008, she was a Lecturer of Physics with the University of Orléans, Orléans, France and a Researcher with LPC2E/CNRS, Orléans, France. Her research works started at LPC2E (Laboratoire de Physique et Chimie de l'Environnement et de l'Espace) in 1994 in the team atmosphere. She is a Professor of Physics with the Observatoire des Sciences de l'Univers région Centre, University of Orléans, Orléans, France, since 2008. She is a confirmed Scientist and has experience in coordinating national project and has been Co-Investigator in European projects (HIBISCUS, SCOUT-O3) and was involved in Satellite Validation Group for chemical measurements (MIPAS or ACE instrument for example). Currently, she is involved in the TARANIS space mission for studying the chemical impact of TLE (blue jet and sprites) on ozone and NOy content in the stratosphere/mesosphere. Her research interests include atmospheric science, which lie mainly in modeling of chemical behavior in the atmosphere (MIPLASMO model).